2024 SICASH
SLIIT INTERNATIONAL CONFERENCE ON ADVANCEMENTS IN SCIENCES & HUMANITIES

Physicochemical Properties of a Brick Made from Clay Brick Waste/Cement/Rice Husk Ash – Insights from the Microstructure and FTIR Analyses

W.D.C.C. Wijerathne*[1], R.L. Samaraweera[2], R.P.T.N. Rajapaksha[3]

[1,2,3]*Uva Wellassa University of Sri Lanka*

Email address of the corresponding author – *chathura@uwu.ac.lk

Abstract

Masonry units (i.e., bricks or earth blocks) made from agro and demolition waste have become popular day-by-day as a sustainable solution for environmental pollution. At the same time, such developments are also proposed as "adsorptive units" to treat heavy metals and organic dyes in industrial effluent streams. In this regard, a brick made from rice husk ash/cement/clay brick waste has been proposed to serve as both a masonry and adsorptive unit with a compressive strength of 3.61 MPa and 51% water absorption, which is suitable for non-load-bearing applications and can effectively adsorb common pollutants in wastewater (i.e. Pb(II), Hg(II), As(V)). However, the reported adsorption and mechanical properties have not been linked with the brick's microstructure and surface characteristics. Thus, an in-depth understanding of the brick's performance is unclear. In this regard, the present study utilizes Scanning Electron Microscopy (SEM) and Fourier Transformation Infrared Spectroscopy (FTIR) techniques to investigate the above. As per study outcomes, a pozzolanic reaction is evident in the brick through SEM and FTIR analyses. The phases portlandite, ettringite and calcium hydroxide phases are visible in the brick after 28 days of development, and the brick's physical properties (water absorbency and compressive strength) can be correlated with C-S-H and C-A-H phases. Based on FTIR studies, it is evident that active groups (O-H and C-S-H) exist on the brick's surface to assist the adsorption of Hg (II), Pb(II) and As(V) adsorbates.

Keywords: Rice husk ash; Clay brick waste; Brick; Adsorption; FTIR

Introduction

Mitigating environmental pollution has been a growing research area nowadays. In this regard, a substantial effort has been taken to reduce heavy metal and toxic organic dye concentrations in industrial wastewater streams by using abundant, but effective adsorbents such as peanut shells, rice husk ash, rice straw, cassava starch, brick waste etc (Foong et al., 2022; Mokokwe & Letshwenyo, 2022a, 2022b; Tejedor et al., 2020). As these adsorbents are applied as aggregates or powder forms on respective adsorption areas, handling the adsorption process becomes tiresome. Thereby, the need for an "adsorptive unit" which can be conveniently used for adsorption purposes is critical.

Another sustainable use of agricultural, industrial sludge and construction waste is masonry units (i.e., earth blocks or bricks), that can be used in the construction industry. Here, suitable materials such as rice husk, rice husk ash, coconut shells, peanut

https://doi.org/10.54389/GOJH6897

shells, clay brick waste, and rice straw are blended with clay and/or cement for developing masonry units (Erdogmus et al., 2021; Rajapaksha & Wijerathne, 2022). Most of these masonry units usually meet international standards such as ASTM C129 and C90 for load or non-load-bearing walls. However, there existed a critical need to develop a masonry unit by using the aforementioned waste, which is also capable of acting as an "adsorptive unit", to better serve nature.

In this context, a novel brick was proposed recently, which is made of rice husk ash, clay brick waste and cement. This brick has 3.61 MPa compressive strength and 51% (w/w) water absorption (Rajapaksha & Wijerathne, 2021). Furthermore, it is capable of using as an "adsorptive unit" to treat wastewater streams with Pb (II), Hg(II), As(V) ions and Malachite Green (MG) dye with a significant removal efficiency (i.e. 98% for Pb(II), 78% for Hg(II), 22% for As(V) and 99% for Malachaite Green) (Rajapaksha et al., 2022). In the reported studies, the optimum material composition for making the aforementioned brick and its adsorption characteristics have been investigated (Rajapaksha & Wijerathne, 2021; Rajapaksha et al., 2022). However, to date, its mechanical properties have not been correlated with the microstructure. Also, its adsorption characteristics have not been correlated with a surface analysis technique such as FTIR. Therefore, a critical research gap lies in investigating how physicochemical properties (i.e., water absorbency, compressive strength, adsorption characteristics) of such a brick can be correlated with its microstructure and surface properties, which is essential in assessing and optimizing its applications in masonry and wastewater treatment. This research gap will be addressed by this work.

In this manuscript, we first briefly discuss the methodology of brick development and how the characterization experiments have been conducted. Here, Scanning Electron Microscopy (SEM) studies and FTIR analyses are focused as the key characterization experiments in this study. The key results will be presented and discussed next, which will be followed by the conclusions of this study. The areas of future research will be presented finally, to sum up.

Methods

2.1 Development of the brick

The brick was made by using rice husk ash (RHA), clay brick waste (CBW), cement and water. During its construction, five raw material compositions were used to select the optimum mixing ratio (by volume) among materials. Accordingly, the volume ratio among cement: CBW: RHA: water content was used as 2:2:4:1, 2:2:6:1, 2:2:8:1, 2:3:6:1 and 1:3:6:1. Each brick was allowed to settle in a wooden mould (dimensions: 7×5×3 cm) for about 12 h at atmospheric conditions, and they were dried for 10 h in the open air after settling. As detailed in our previous work (Rajapaksha & Wijerathne, 2021), the optimum mixing ratio was chosen by considering the porosity, water absorbency, compressive strength and the ability to remove the brick from the mould. Accordingly, the optimum mixing ratio for cement: CBW: RHA: water was chosen as 2:3:6:1. For this brick, water absorbency and 28-d compressive strength were measured as 51% and 3.61 MPa, respectively (Rajapaksha et al., 2022). To further assess the optimized brick's performance, the adsorption studies were conducted for the brick with this optimum mixing ratio for Pb (II), As(V) and Hg (II).

2.2 Scanning Electron Microscopy (SEM) and Fourier Transform Infrared Spectroscopy (FTIR) analysis

A part of the brick's cross-section was taken, and it was mounted on the stub using double-sided adhesive carbon tape. Then the specimen was gold-coated by (JEOL auto fine coater model JFS -1600) and micrographs were recorded using a Scanning Electron Microscope (ZEISS, EVO LS15). The FTIR spectra for rice husk ash, clay brick waste, cement and the untreated (or un-adsorbed) brick were obtained using a Fourier Transform Infrared Spectrophotometer (FTIR) (Model: Bruker Alpha) in the range of 400 to 4000 cm^{-1} using the attenuated total reflectance (ATR) mode. At the end of adsorption, the FTIR graphs

were also obtained for each adsorbate (i.e., Pb (II), Hg (II) and As(V)) and here, the brick was first dried and then its surface was scratched to get a powdered sample for FTIR analysis.

Resuls & Discussion

3.1 Analysis of the brick's microstructure

Figure 1 qualitatively depicts the phases present in the microstructure of the brick made of cement, RHA, CBW and water after 28 days of its development (i.e., curing time).

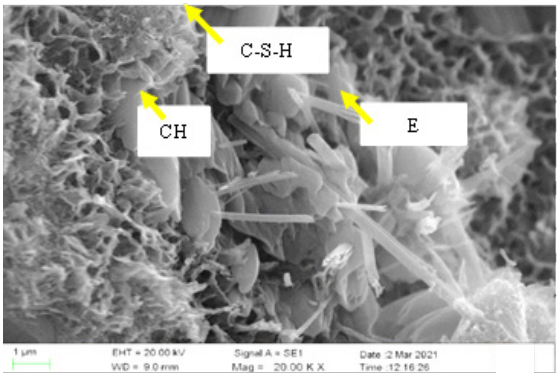

Figure 1: Scanning electron microscopy image for untreated brick

Accordingly, Portlandite (CH or Ca (OH)2) appears as plates and Ettringite (E or Ca6 Al2(SO4)3 (OH)12.26H2O) appears as needle-like crystals (Hamzah et al., 2022). Calcium Silica Hydroxide (C-S-H), which resembles a sponge-like structure, is also observed (Hamzah et al., 2022). To this end, C-S-H could form at the initial stages of hydration and/or as a result of a pozzolanic reaction. However, an SEM coupled with EDX or an FTIR is required to confirm the origin of C-S-H in this context. Furthermore, the existence of Ettringite, Portlandite and Calcium Silica Hydroxide at the end of 28 days is also reported for bricks made of OPC cement (Yun et al., 2019), which aligns with the current finding.

3.2 Relationship between brick's microstructure and physical properties

Table 1 compares the water absorbency and compressible strength values of different bricks chosen from the literature with this work. To obtain further insights, we also included the results obtained by using an RHA-free brick (i.e. 0%).

Table 1. Water absorption and compressive strength of different brick samples (RHA: Rice husk ash, CBW-Clay brick waste)

Brick composition (weight %)	Compressive strength (MPa)	Water absorption (%)	Ref.
8% RHA + 56% CBW + cement	3.61 (28d strength)	51.0	This work
0% RHA + 51% CBW + cement	3.61 (28d strength)	20.0	
10% RHA + clay (fired)	4.45	15.56	(Mohan et al., 2012)
10% RHA + clay (fired)	1.81	27	(Perera et al., 2015)
4% RHA + clay (fired)	3.55	19.51	
0% RHA + clay (fired)	2.68	21	
10% RHA + cement + aggregates	3.93±0.12 (14d strength)	NA	(Tram, 2017)
0% RHA + cement + aggregates	4.97±0.31 (14d strength)	NA	
10% RHA + lime + cement (weight % is given with respect to cement)	3.47 (28d strength)	19.896	(Pushpakumara & De Silva, 2012)
10% RHA + lime + cement	4.94 (28d strength)	NA	
Commercial clay brick (100% clay)	2.7	NA	(Fernando, 2017)

Accordingly, the RHA/CBW/Cement brick shows a water absorbency of 51%, which is about 30% lower when the brick is made without RHA. Thereby, RHA may contribute to higher water absorption, which could be due to its high porosity (Fernando, 2017; Hwang & Huynh, 2015b). However, the corresponding water absorbency values do not vary much for clay/RHA bricks with 0%, 4% and 10% of RHA (see Table 1). Now, due to the reaction between Al_2O_3 in CBW with lime in cement, calcium aluminate hydrate (C-A-H) can also form. As C-S-H and C-A-H gels demonstrate

water absorption potential (Maierhofer et al., 2010), the aforementioned increase in water absorbency may take place in bricks when RHA and CBW are used with cement.

It is known that the porosity, pore size and type of crystallization govern the compressive strength of a brick (Fernando, 2017). By referring to Table 1, the compressive strength of commercial pure clay brick is around 2.7 MPa, and some works reported a similar value during experiments for fired clay brick. Possibly due to the additional cement content, the developed brick possesses a higher strength compared to 100% clay brick (i.e., 3.61 MPa). As per the literature, the compression strength usually decreases with the RHA content due to the high porosity of RHA (Hwang & Huynh, 2015a). For fired clay/RHA bricks, recrystallization of the RHA structure during sintering also leads to a decrease in compressive strength (Fernando, 2017; Perera et al., 2015). However, in this work, where firing was not used, the compressive strength remained the same even after RHA was added. To this end, the compressive strength was reported as increasing with the curing time, and the rate of increase is higher in RHA mixed cement concrete, compared to 0% RHA samples (Ettu et al., 2013). They correlated this observation with the formed C-S-H gel that can increase binder efficiency.

As per Figure 1, the formation of the C-S-H gel is evident in the developed brick. Moreover, as RHA also gives pozzolans to the brick in the form of SiO_2, the amount of C-S-H formed should be high compared to a clay/RHA brick. Furthermore, the C-A-H gel also increases binder efficiency. The overall formation of C-S-H and C-A-H may lead to compensation for the strength reduction due to the porosity of RHA. However, further research is required to uncover the key player(s) herein.

3.3 Fourier transform infrared spectroscopy (FTIR) analyses of raw materials and untreated brick

Figure 2 shows the FTIR graphs obtained for rice husk ash (RHA), clay brick waste (CBW), OPC cement and the developed brick.

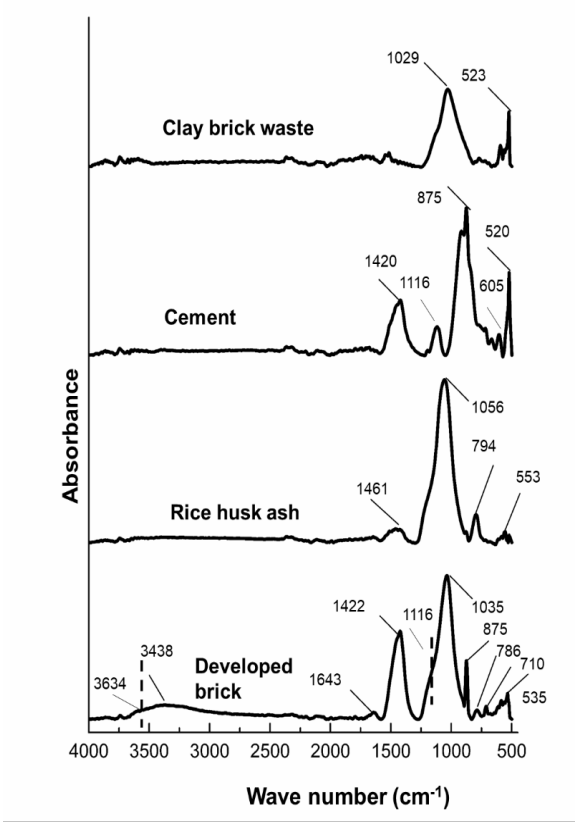

Figure 2: FTIR graphs for cement, rice husk ash (RHA), clay brick waste (CBW) and untreated brick.

Accordingly, for RHA, the peak around 794 cm^{-1} is possibly due to the vibration of symmetrical stretching of the Si-O-Si bond, while the intense absorption around 1056 cm^{-1} corresponds to the stretching of asymmetric Si-O-Si bonds (Nascimento, 2020). However, the broad peak around 3400 cm^{-1} is not visible in this RHA sample (corresponds to adsorbed water), which could be due to the drying of the sample before analysis.

Furthermore, the stretching of Si-O and Al-O-Si bonds is evident in clay brick waste through peaks around 1029 cm^{-1} and 523 cm^{-1} (Govindasamya et al., 2019). Considering OPC cement, the in-plane-bending and asymmetric stretching of C-O bonds in CO_3^{2-} is evident through peaks at 1420 cm^{-1} and 875 cm^{-1}, while the symmetric stretching of Si-O bonds in the Ettringite phase corresponds to peak at 1116 cm^{-1} (Tararushkin et al., 2020). The out-of-plane bending vibration of Si-O bonds corresponds to the sharp peak at 520 cm^{-1}

(Tararushkin et al., 2020). For the developed brick, new peaks are observed at 3438 cm^{-1}, 1643 cm^{-1} and 710 cm^{-1}. The peak at 875 cm^{-1} remains the same while making it sharper.

The broad peak at 3438 cm^{-1} can be attributed to the symmetric stretching of water molecules on the brick's surface (Sivakumar & Ravibaskar, 2009). The peak at 710 cm^{-1} can be ascribed to the out-of-plane bonding of C-O bonds in CO_3^{2-}. In addition, the stretching vibration of Al-O bonds can be correlated with the peaks in the 600 – 700 cm^{-1} region (Jose et al., 2020). The new peak observed at 1643 cm^{-1} can be attributed to the bending vibration of O-H groups (Jose et al., 2020). The research reports the existence of Ca $(OH)_2$ through a sharp peak around 3628 -3634 cm^{-1} (Horgnies et al., 2013; Jose et al., 2020). This peak is not profound for the developed brick but can be observed in the shoulder region. A prominent peak observed for the Ettringite phase in OPC cement (as a raw material) is also visible in the shoulder region (dashed line). Moreover, the peak at 1035 cm^{-1} can be attributed to the C-S-H that formed due to pozzolanic reactions (Jose et al., 2020; Sumesh et al., 2019). Thereby, it is evident that CBW and/or rice husk ash acted as pozzolanic material(s) in corresponding reactions.

3.4 Fourier transform infrared spectroscopy (FTIR) analyses of treated brick with different adsorbates

As per Figure 3, which shows the FTIR graphs obtained for the untreated brick and treated bricks, a broad peak (corresponding to the stretching of the O-H bond) around 3383 cm^{-1} for the untreated brick, shifts to 3387 3385 and 3385 cm^{-1} for Pb(II), Hg(II) and As(V), respectively. However, the intensity of the peak is very insignificant for As(V), and the peak shift can be considered as little. A similar minor shift is observed for the peaks assigned to in-plane and out-of-plane bending of C-O bonds in CO_3^{2-} (1410 cm^{-1} and 712 cm^{-1}) for all adsorbates. Furthermore, no peak shift is observed for asymmetric stretching of C-O bonds (873 cm^{-1}).

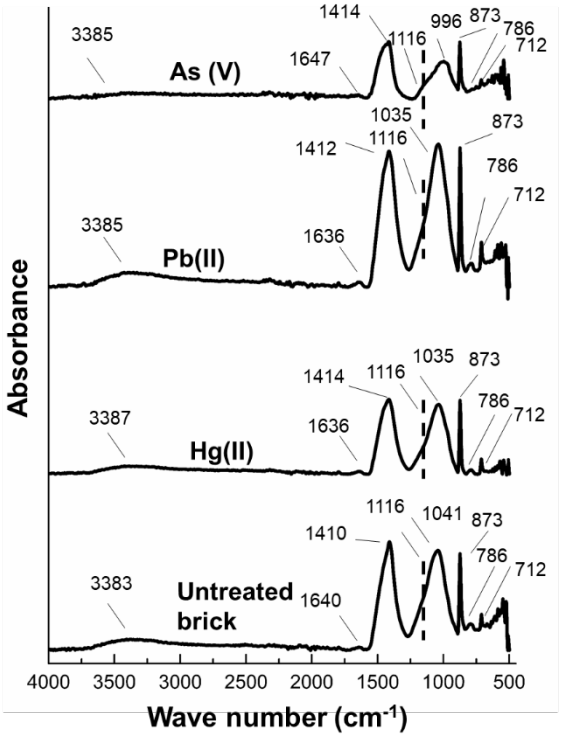

Figure 3: FTIR graphs obtained for the brick for the contact with different adsorbates

However, the shift of the O-H bending peak (1640 cm^{-1}) for all adsorbates is significant. In fact, the peak intensity is fewer for As(V) indicating the significant reduction of O-H groups on the brick's surface after adsorption. In addition, the peak corresponding to C-S-H significantly shifts to wave numbers 1035 and 996 cm^{-1}, indicating a higher contribution to the adsorption process. To this end, a recent study reports possible electrostatic interactions between C-S-H gel and ions during adsorption (Zhang et al., 2022).

As per the peak shifts observed in the FTIR graph, it is evident that the adsorbent (i.e., brick) has active sites on its surface (i.e. O-H and C-S-H) that can facilitate ion adsorption. Furthermore, the contribution of Si-O-Si, Si-O, CO and C-O groups to adsorption is negligible, which contradicts the reported adsorption sites of Hg (II) and/or Pb(II) in similar adsorbents (without cement). Nevertheless, the As(V) adsorption is found to be affected by O-H groups on the adsorbent surface (Zeng et al., 2020). Furthermore, as the adsorption study was conducted

on the surface of the brick, more studies are required to investigate the adsorption phenomenon in the brick's interior to obtain further insights.

Conclusions

This work focuses on the surface level and microstructural characterization of a novel brick made from rice husk ash/cement/clay brick waste. As per study outcomes, a pozzolanic reaction is evident in the brick. The phases portlandite, ettringite and calcium hydroxide are visible in the brick after 28 days of development, and the brick's physical properties (water absorbency and compressive strength) can be correlated with the existence of C-S-H and C-A-H phases. As per FTIR studies, it is evident that active groups (-OH and C-S-H) exist on the brick's surface to assist the adsorption of Hg(II), Pb(II) and As(V) adsorbates.

Acknowledgement

The authors would like to thank the technical staff of the Faculty of Technology, Rajarata University of Sri Lanka, Faculty of Applied Sciences and Uva Wellassa University for facilitating analytical tests.

References

Erdogmus, E., Harja, M., Gencel, O., Sutcu, M., & Yaras, A. (2021). New construction materials synthesized from water treatment sludge and fired clay brick wastes. Journal of Building Engineering, 42, 102471.

Ettu, L., Ajoku, C., Nwachukwu, K., Awodiji, C., & Eziefula, U. (2013). Strength variation of OPC-rice husk ash composites with percentage rice husk ash. Int J Appl Sci Eng Res, 2(4), 421-424.

Fernando, P. (2017). Experimental investigation of the effect of fired clay brick on partial replacement of rice husk ash (RHA) with brick clay. Advances in Recycling and Waste Management, 2(1), 1-4.

Foong, S. Y., Chan, Y. H., Chin, B. L. F., Lock, S. S. M., Yee, C. Y., Yiin, C. L., Lam, S. S. (2022). Production of biochar from rice straw and its application for wastewater remediation– An overview. Bioresource Technology, 360, 127588.

Govindasamya, A., Viruthagiri, G., & Ramesh, K. (2019). FT-IR Spectroscopic and Porosity Studies to Estimate the Firing Temperature of the Clay Brick. International Journal of Applied Engineering Research, 14(12), 2904-2909.

Hamzah, N., Mohd Saman, H., Baghban, M. H., Mohd Sam, A. R., Faridmehr, I., Muhd Sidek, M. N.,. Huseien, G. F. (2022). A review on the use of self-curing agents and its mechanism in high-performance cementitious materials. Buildings, 12(2), 152.

Horgnies, M., Chen, J., & Bouillon, C. (2013). Overview about the use of Fourier transform infrared spectroscopy to study cementitious materials. WIT Trans. Eng. Sci, 77, 251-262.

Hwang, C.-L., & Huynh, T.-P. (2015a). Evaluation of the performance and microstructure of ecofriendly construction bricks made with fly ash and residual rice husk ash. Advances in Materials Science and Engineering, 2015.

Hwang, C.-L., & Huynh, T.-P. (2015b). Investigation into the use of unground rice husk ash to produce eco-friendly construction bricks. Construction and Building Materials, 93, 335-341.

Jose, A., Nivitha, M., Krishnan, J. M., & Robinson, R. (2020). Characterization of cement stabilized pond ash using FTIR spectroscopy. Construction and Building materials, 263, 120136.

Maierhofer, C., Reinhardt, H.-W., & Dobmann, G. (2010). Non-destructive evaluation of reinforced concrete structures: non-destructive testing methods. Elsevier.

Mohan, N. V., Satyanarayana, P., & Rao, K. S. (2012). Performance of rice husk ash bricks. International Journal of Engineering Research and Applications, 2(5), 1906-1910.

Mokokwe, G., & Letshwenyo, M. W. (2022a). Investigation of clay brick waste for the removal of copper, nickel and iron from aqueous solution: batch and fixed–bed column studies. Heliyon, 8(7).

Mokokwe, G., & Letshwenyo, M. W. (2022b). Utilisation of cement brick waste as low cost adsorbent for the adsorptive removal of copper, nickel and iron from aqueous solution: Batch and column studies. Physics and Chemistry of the Earth, Parts A/B/C, 126, 103156.

Nascimento, A. C. K. (2020). Study of rice husk ash by infrared spectroscopy. Int. J. Sci. Eng. Investig, 9, 60-62.

Perera, B., Madhushanka, G., De Silva, G., & De Silva, G. (2015). Effect of rice husk ash (RHA) on structural properties of fired clay bricks. 6th International Conference on Structural Eng. and Construction Management.

Pushpakumara, B., & De Silva, G. (2012). Characteristics of masonry blocks manufactured with rice husk ash (RAH) and lime.

Rajapaksha, R.P.T.N., & Wijerathne, W.D.C.C. (2021). Investigating the potential of clay brick waste to be used as a raw material for rice husk ash-based bricks.

Rajapaksha, R.P.T.N., & Wijerathne, W.D.C.C. (2022). Use of agro-waste for masonry unit construction in Sri Lanka: A mini-review International Research Symposium 2022, University of Vocational Technology, Sri Lanka.

Rajapaksha, R.P.T.N., Wijerathne, W.D.C.C., & Rambukwella, I.A. (2022). A novel brick made from clay brick waste/rice husk ash/cement to adsorb heavy metals and organic dyes in wastewater. 2022 Moratuwa Engineering Research Conference (MERCon).

Sivakumar, G., & Ravibaskar, R. (2009). Investigation on the hydration properties of the rice husk ash cement using FTIR and SEM. Applied Physics Research, 1(2), 71-77.

Sumesh, M., Alengaram, U. J., Jumaat, M. Z., & Mo, K. H. (2019). Microstructural and strength characteristics of high-strength mortar using nontraditional supplementary cementitious materials. Journal of Materials in Civil Engineering, 31(4), 04019017.

Tararushkin, E., Shchelokova, T., & Kudryavtseva, V. (2020). A study of strength fluctuations of Portland cement by FTIR spectroscopy. IOP Conference Series: Materials Science and Engineering.

Tejedor, J., Cóndor, V., Almeida-Naranjo, C., Guerrero, V., & Villamar, C. (2020). Performance of wood chips/peanut shells biofilters used to remove organic matter from domestic wastewater. Science of The Total Environment, 738, 139589.

Tram, N. X. T. (2017). Utilization of Rice Husk Ash as partial replacement with Cement for production of Concrete Brick. MATEC Web of Conferences.

Yun, H.-D., Lee, J.-W., Jang, Y.-I., Jang, S.-J., & Choi, W. (2019). Microstructure and mechanical properties of cement mortar containing phase change materials. Applied Sciences, 9(5), 943.

Zeng, H., Zhai, L., Qiao, T., Yu, Y., Zhang, J., & Li, D. (2020). Efficient removal of As (V) from aqueous media by magnetic nanoparticles prepared with Iron-containing water treatment residuals. Scientific Reports, 10(1), 9335.

Zhang, Y., Yang, Z., & Jiang, J. (2022). Insight into ions adsorption at the C-S-H gel-aqueous electrolyte interface: From atomic-scale mechanism to macroscopic phenomena. Construction and Building materials, 321, 126179.